

Analysis of Moving Dielectric Half-Space with Oblique Plane Wave Incidence Using the Finite Difference Time Domain Method

Mohammad Marvasti and Halim Boutayeb*

Abstract—We propose an original and detailed investigation of a moving dielectric half-space with oblique plane wave incidence, by using the Finite Difference Time Domain (FDTD) method. In our FDTD program, movements are implemented by changing positions of the interfaces at different time instants, through the classical FDTD time loop. With this “brute-force” approach, time is implicitly absolute, and Voigt-Lorentz transformations are not implemented. This technique is suitable for non-relativistic electromagnetic problems with moving bodies, thus for most encountered electromagnetic problems. We analyze the transmitted and reflected waves, for different speeds, different refractive indices, and different incidence angles. Based on the obtained results, we derive several analytical formulas for the reflection coefficients, transmission coefficients, Doppler frequency shifts, and angles of transmission and reflection. These formulas are validated by full-wave electromagnetic simulations and are in agreement with the literature. The electric field distribution obtained at time instants is also studied.

1. INTRODUCTION

Maxwell’s equations encompass the main laws of electromagnetism. The Finite Difference Time Domain (FDTD) method is a rigorous and powerful tool for modeling electromagnetic devices. FDTD solves Maxwell’s equations directly without any physical approximation, and the maximum problem size is limited only by the extent of the computing power available. The FDTD method is based on the discretization of Maxwell’s equations in time and space domains. Invented in 1966 [1], it is applied for the first time in 1975 to study the effect of electromagnetic radiation on human eyes [2]. A microstrip patch antenna is analyzed in the time domain in 1989, by using FDTD [3]. In 1990, the FDTD technique is used for the first time for microwave circuits [4]. In 1991, an algorithm is proposed to obtain the electromagnetic radiation in far field from near field results, in FDTD code [5]. Today, the FDTD method is used in a wide range of applications from DC to optics.

The problem of the interaction of electromagnetic waves with moving media has been an important subject of interest for a long time, due to its wide application in many domains such as radio sciences, optics, and astrophysics. Numerous investigations have been carried out in this area, which is interesting from a practical and theoretical point of view. In the microwave domain, the study of electromagnetic problems with moving dielectric media is useful in many applications such as, for example, radar systems for the detection of vital signs [6, 7] or time-varying waveguides [8]. In [9], the authors present a method based on the concept of propagators for analyzing the reflection and transmission of obliquely incident electromagnetic waves by a moving slab. The proposed propagators map the total field at any point inside the slab, to the fields on the left-hand side boundary of the slab. In [10], Voigt-Lorentz transformations are used to obtain formulas for the intensity of the reflected and transmitted

Received 22 January 2023, Accepted 16 February 2023, Scheduled 22 February 2023

* Corresponding author: Halim Boutayeb (halim.boutayeb@uqo.ca).

The authors are with the Department of Electrical Engineering, University of Quebec, 101 rue Saint-Jean Bosco, Gatineau (Qc) J8X 3X7, Canada.

wave when electromagnetic radiation is incident on a moving dielectric slab. In [11], the reflection and transmission of a plane wave, with its electric vector polarized in the plane of incidence, by a moving dielectric slab are investigated theoretically. Two cases of movement are considered: the dielectric slab moves parallel to the interface, or the dielectric slab moves perpendicular to the interface. In [12], the problem of the propagation of modes along a moving dielectric interface is considered, using a moving dielectric slab or a moving dielectric circular cylinder. In [13], the reflection of electromagnetic waves from a moving dielectric half-space is investigated for parallel and perpendicular motions of a dielectric medium. The paper [14] deals with the scattering of electromagnetic waves from a moving dielectric cylinder illuminated by an oblique incident of the plane wave, by using the three-dimensional Finite Element Method (FEM).

The FDTD method has been successfully used for analyzing electromagnetic problems with moving bodies [15–24]. In [17], the authors propose a technique based on integrating Voigt-Lorentz transformations in FDTD. In this work, the implementation of movements is done by changing the positions of bodies at each cycle of the FDTD time loop. With this “brute-force” approach, time is implicitly absolute and Voigt-Lorentz transformations are not implemented. This technique is suitable for non-relativistic electromagnetic problems with moving bodies, thus for most encountered electromagnetic problems. We analyze the transmitted and reflected waves of moving dielectric half-space with oblique plane wave incidence. Based on the obtained numerical solutions, we derive several analytical formulas for the transmission coefficients, reflection coefficients, Doppler frequency shifts, and angles of transmission and reflection. These formulas are validated through full-wave simulations.

The remainder of the paper is structured as follows: Section 2 describes the setup used for our FDTD simulations. Section 3 presents the analysis of the obtained numerical results. Finally, concluding remarks are given in Section 4.

2. NUMERICAL SETUP

2.1. Windowed Sine Excitation

For precise detection of the frequency variation and the Doppler effect, we decide to consider as the exciting source a windowed Sine signal $E_i(t) = \Pi(\frac{f_0}{N}t) \sin(2\pi f_0 t)$, presenting a modulated sinusoid $E_i(f) = \frac{N}{f_0} \text{Sinc}(\frac{f-f_0}{Nf_0})$ spectrum, where f_0 is the frequency of excitation and N is the number of periods of Sine function considered for simulation. As it is shown in this paper, this type of excitation provides a sharp frequency spectrum and makes frequency identification accurate and simple.

2.2. Parameters of Discretization

The FDTD space mesh needs to be sufficiently small in order to measure the effect of a moving body. Similarly, the FDTD time step needs to be sufficiently small to be able to detect the smallest velocity considered in the problem. Moreover, due to numerical dispersion, the phase velocity of the wave changes with the angle in the computational volume [25]. This effect decreases by reducing the size of the space mesh. For example with $\delta_x = \frac{\lambda}{40}$ the maximum of velocity change is 0.05% as described in page 35 of [25]. We choose $\delta_x = 0.4$ mm, $\delta_t = 1.8295$ ns, and the wavelength is about 30 mm for our FDTD code in this paper.

2.3. Undesirable Effects Due to Discontinuous Motion of Dielectric Interface

Due to the space discretization in the classical FDTD numerical method, the dielectric interface location does not change continuously because it does not move inside a cell. Instead, in our FDTD code, for a specific value of interface motion speed v , the position of the dielectric interface is fixed for $n\delta_t$ with $n = \lfloor \frac{\delta_x}{v\delta_t} \rfloor$. $\lfloor \cdot \rfloor$ stands for floor function. δ_t and δ_x are the time step and space mesh. Then, after this time, the dielectric interface moves one cell in the desired direction. Fig. 1 shows the discontinuous movement of the source in the FDTD algorithm. Based on our FDTD simulations, we can observe undesirable effects due to the discontinuous movement, generating waves at high frequencies. These

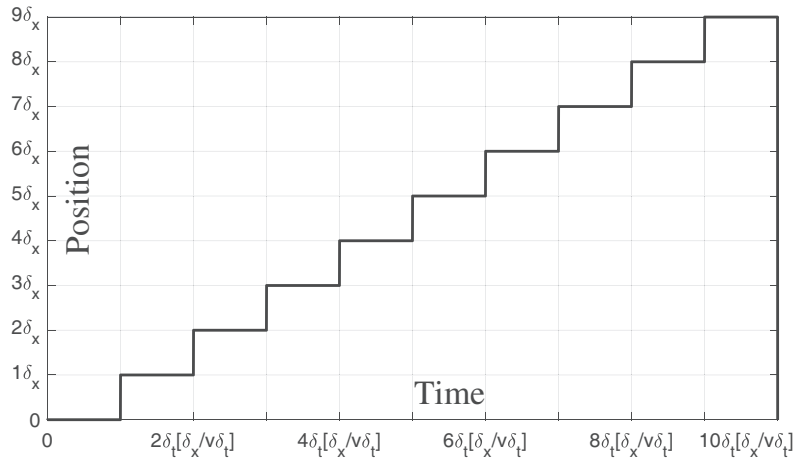


Figure 1. Discontinuous movement of the dielectric interface.

frequencies correspond to wavelengths that are multiple of the space mesh. These undesirable effects can be mitigated by using a small space mesh and a small time step.

2.4. Boundary Conditions

For the problems considered, as illustrated in Fig. 2, we use Perfect Matched Layers (PMLs) in all boundaries except in boundaries parallel to xoy -plane, where only PECs are used.

3. ANALYSIS

3.1. Structure

Figure 2 shows the configuration considered. A plane wave illuminates, at oblique incidence, a dielectric half-space at rest or moving in $-x$ direction toward the source with speed v . The plane wave source is made of z -polarized electric current sources. The dielectric medium has the refractive index n . The plane wave propagates with speed

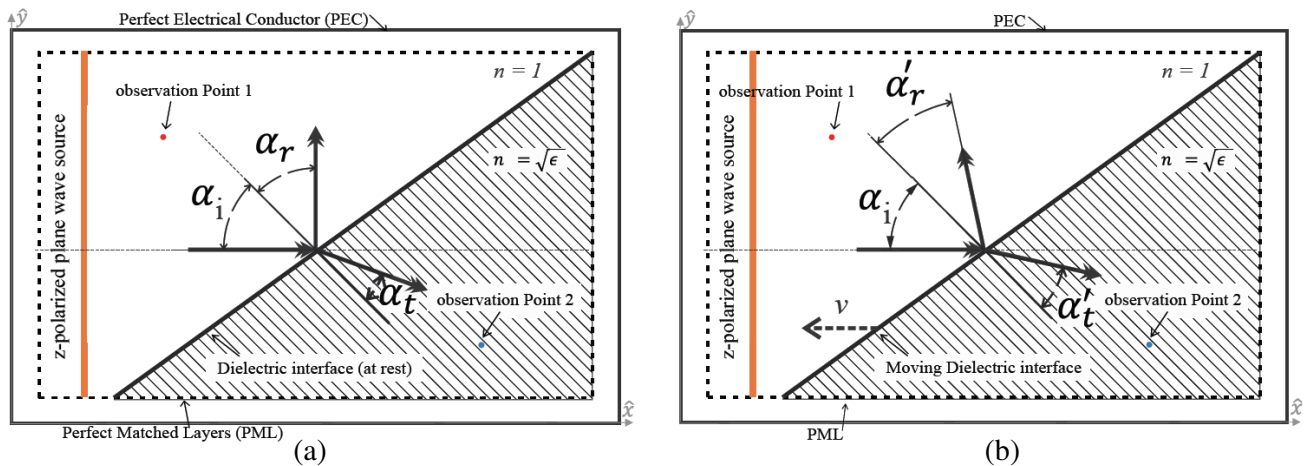


Figure 2. FDTD setup for the analysis of moving dielectric half-space illuminated by a plane wave at oblique incidence. (a) Dielectric interface at rest. (b) Moving dielectric interface.

c in the air toward the interface. Two observers are used to measure the electric field component in the z -axis of the reflected and transmitted waves.

α_i is the angle of incidence. α'_r and α_r are angles of reflected waves, for the moving interface and for the interface at rest, respectively. α'_t and α_t are angles of transmitted waves, for the moving interface and for interface at rest, respectively.

3.2. Field Distribution

Simulated electric field distributions for different values of v/c and different values of n are illustrated in Fig. 3. Results are presented for speeds v close to c only for the purpose of obtaining a better visualization of the Doppler effects. In practical applications, this FDTD method will be used for non-relativistic speeds.

From Fig. 3, the Doppler effect can be observed by analyzing the wavelengths of reflected and transmitted waves. It can be noted that the index n has an effect on the Doppler effect for the transmitted wave but not on the Doppler effect for the reflected wave. We can also see the effect of n

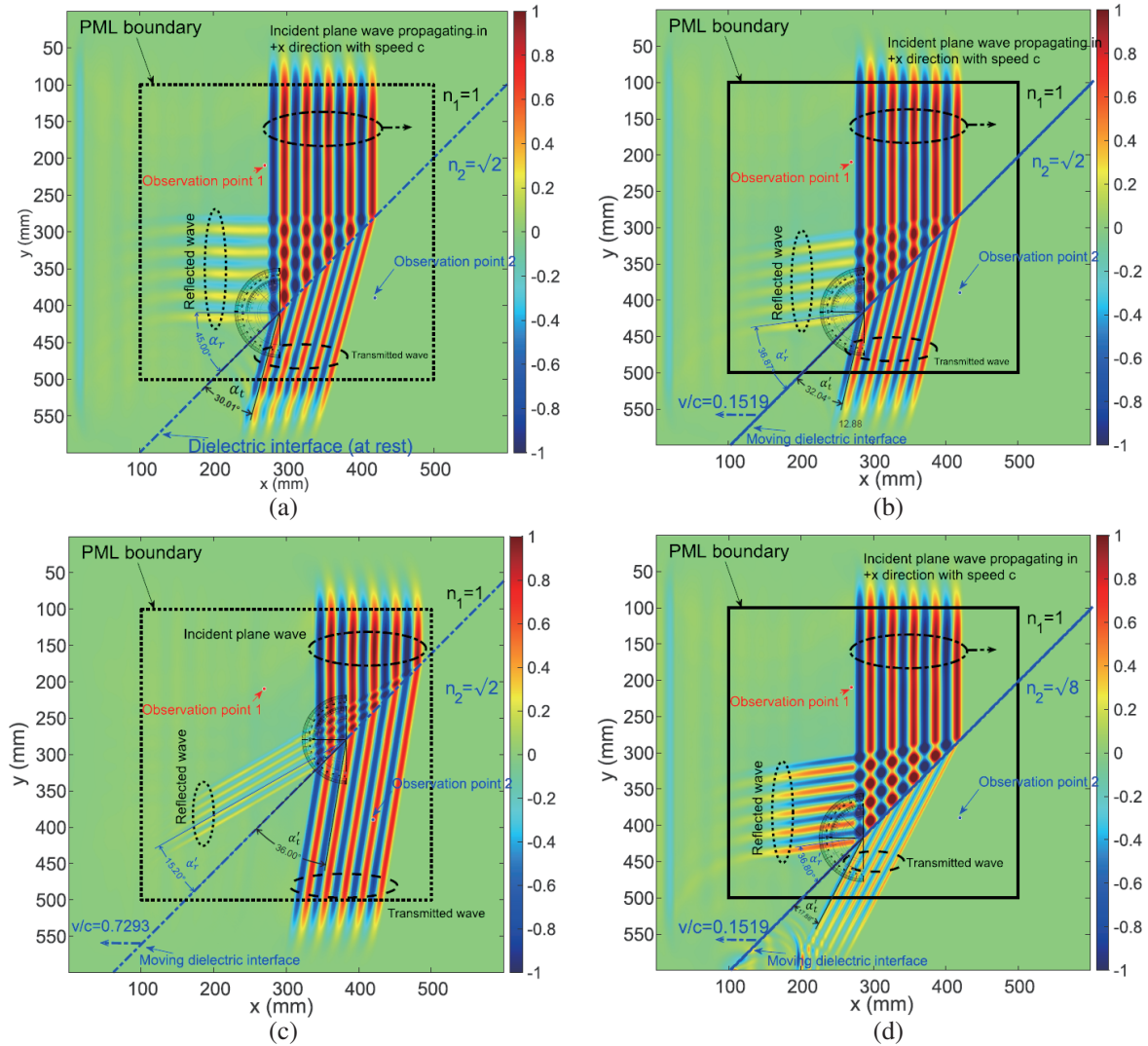


Figure 3. Electric field distributions for dielectric interface with different indices n , moving toward the source at different speeds v . (a) $\frac{v}{c} = 0$ and $n = \sqrt{2}$. (b) $\frac{v}{c} = 0.15$ and $n = \sqrt{2}$. (c) $\frac{v}{c} = 0.72$ and $n = \sqrt{2}$. (d) $\frac{v}{c} = 0.15$ and $n = \sqrt{8}$.

on the amplitudes and angles of reflected and transmitted waves. Fig. 3 shows how we have measured the different angles, with a numerical protractor. By carrying out a series of FDTD simulations and by analyzing the results, different formulas are derived in the next subsections.

3.3. Angles of Reflection and Transmission

The simulated transmission and reflection angles are plotted in Fig. 4 for different values of v/c and for different values of n . We would like to note again that results for speeds v close to c are presented in Fig. 4, only for the purpose to derive formulas from the FDTD simulations. In practical applications, this FDTD method will be used for non-relativistic speeds only. When the dielectric interface is at rest, the reflection angle is

$$\alpha_r = \alpha_i \tag{1}$$

Based on FDTD results (Fig. 4), for the interface moving in $-x$ direction (toward the source), the reflection angle is given by

$$\alpha'_r = 2 \arctan \left(\frac{\tan(\alpha_i)}{1 + \frac{v}{c}} \right) - \alpha_i \tag{2}$$

This is in agreement with the reflection angle obtained for moving metallic reflector illuminated at oblique incidence, in the literature, by using classical electromagnetism. If the interface moves in x direction (away from the source), the reflection angle becomes

$$\alpha'_{r2} = 2 \arctan \left(\frac{\tan(\alpha_i)}{1 - \frac{v}{c}} \right) - \alpha_i \tag{3}$$

When the dielectric interface is at rest, based on Snell-Descartes law and confirmed by FDTD, the transmission angle is

$$\alpha_t = \arcsin \left(\frac{\sin(\alpha_i)}{n} \right) \tag{4}$$

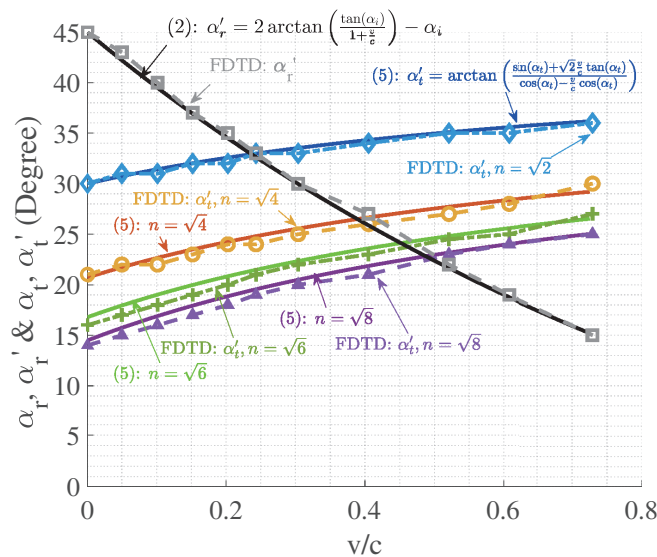


Figure 4. Simulated angles of transmitted and reflected waves for dielectric interface moving toward the source, with incidence angle $\alpha_i = 45^\circ$, versus $\frac{v}{c}$. Comparison with derived analytical formulas. Other incidence angles were also tested (not shown here).

Based on FDTD results (Fig. 4), for the interface moving in $-x$ direction (toward the source), the transmission angle is given by

$$\alpha'_t = \arctan \left(\frac{\sin(\alpha_t) + n \frac{v}{c} \tan(\alpha_t)}{\cos(\alpha_t) - \frac{v}{c} \cos(\alpha_t)} \right) \quad (5)$$

3.4. Doppler Frequency Shifts and Amplitudes for Reflected Waves

Figure 5 shows the reflected signal in the frequency domain, for different values of v/c . These results are used to analyze how the frequency and amplitude vary as functions v/c . The effect of n is also considered in the analyses. We call f'_r the frequency of the reflected wave when the interface is moving and f the frequency when the interface is at rest. A'_r and A_r are the amplitudes of reflected waves in the frequency domain, for the moving interface and for the interface at rest, respectively.

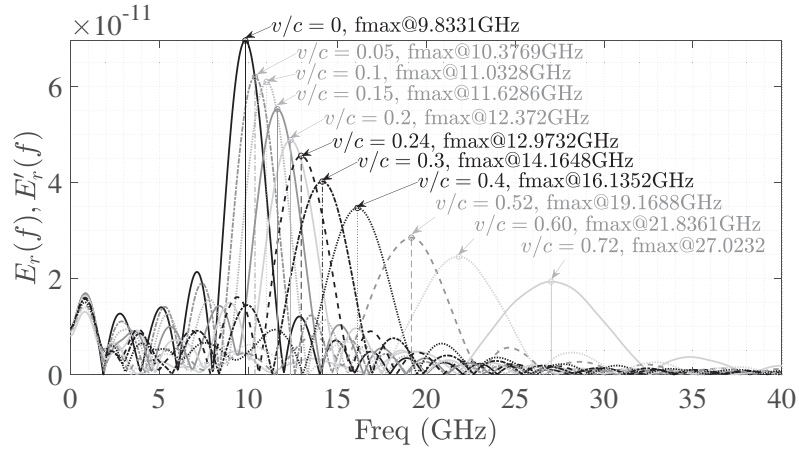


Figure 5. Simulated amplitude of reflected wave in the frequency domain, for dielectric interface moving toward the source, with incidence angle $\alpha_i = 45^\circ$, for different values of $\frac{v}{c}$ ($\epsilon_r = 2$).

As shown in Fig. 6, the Doppler frequency shift for the reflected wave is given by

$$\frac{f'_r}{f} = \frac{\sin(\alpha_i)}{\sin(\alpha'_r)} \quad (6)$$

Figure 7 shows how this formula is derived geometrically.

We have also obtained the following formula for the amplitude of the reflected wave:

$$\frac{A'_r}{A_r} = \frac{\cos\left(\frac{\alpha'_r + \alpha_i}{2}\right) - n \sin(\alpha'_r + \alpha_i)}{\cos\left(\frac{\alpha'_r + \alpha_i}{2}\right) + n \sin(\alpha'_r + \alpha_i)} \times \frac{\cos(\alpha_i) + n \sin(2\alpha_i)}{\cos(\alpha_i) - n \sin(2\alpha_i)} \times \frac{\sin(\alpha'_r)}{\sin(\alpha_i)} \quad (7)$$

For normal incidence, the Doppler effect formula and the amplitude ratio are simplified by:

$$\frac{f'_r}{f} = \frac{A_r}{A'_r} = \frac{1 + \frac{v}{c}}{1 - \frac{v}{c}} \quad (8)$$

This is the same formula obtained with classical electromagnetism or with special relativity for moving reflectors illuminated at normal incidence. This further validates the proposed FDTD approach.

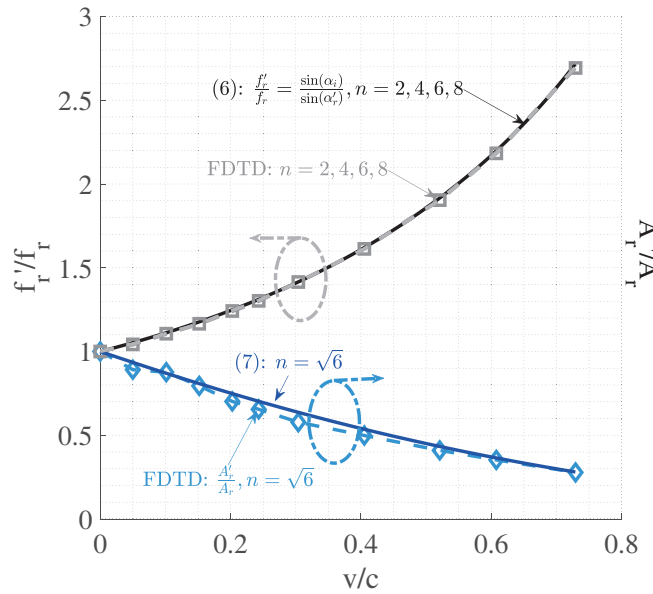


Figure 6. Simulated amplitude in the frequency domain and frequency of reflected waves, for dielectric interface moving toward the source, with incidence angle $\alpha_i = 45^\circ$, versus $\frac{v}{c}$. Comparison with derived analytical formulas.

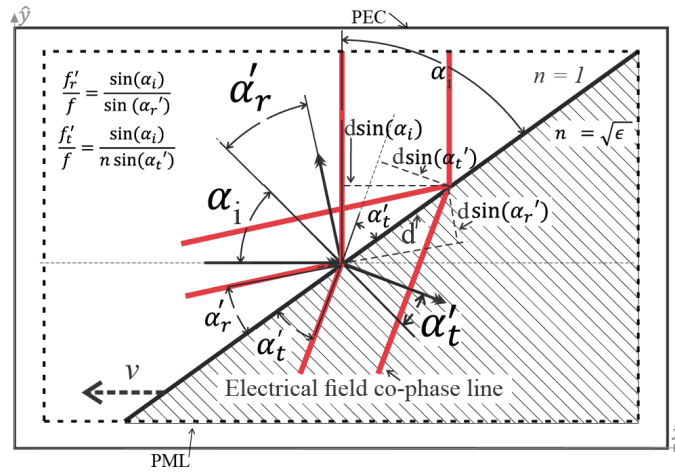


Figure 7. Geometrical method used to derive the Doppler effect formulas for reflected and transmitted waves.

3.5. Doppler Frequency Shifts and Amplitudes for Transmitted Waves

The transmitted waves, in the frequency domain, obtained with FDTD for different values of v/c are plotted in Fig. 8. f'_t is the frequency of the transmitted wave when the interface is moving and f the frequency when the interface is at rest. A'_t and A_t are the amplitudes of transmitted waves in the frequency domain, for the moving interface and for interface at rest, respectively. As shown in Fig. 9, the Doppler frequency shift for the transmitted wave is given by

$$\frac{f'_t}{f} = \frac{\sin(\alpha_i)}{n \sin(\alpha'_t)} \tag{9}$$

Again, Fig. 7 shows how this formula is derived geometrically. The amplitude of the transmitted

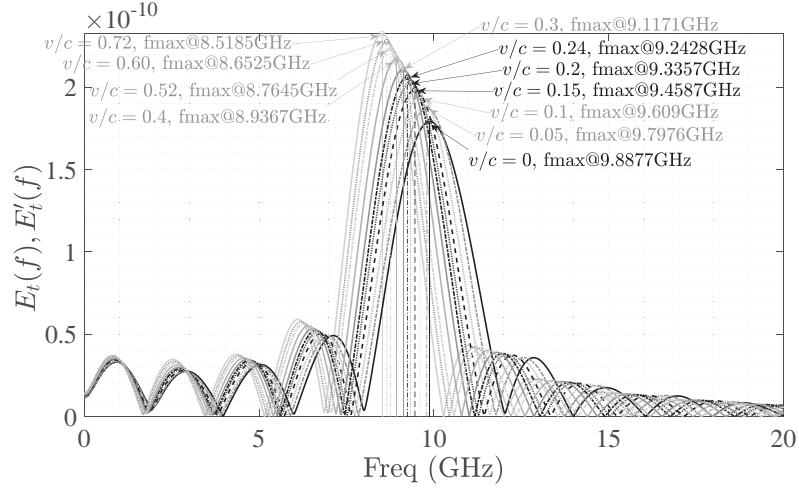


Figure 8. Simulated amplitude of transmitted wave in the frequency domain, for dielectric interface moving toward the source, with incidence angle $\alpha_i = 45^\circ$, for different values of $\frac{v}{c}$ ($\epsilon_r = 2$).

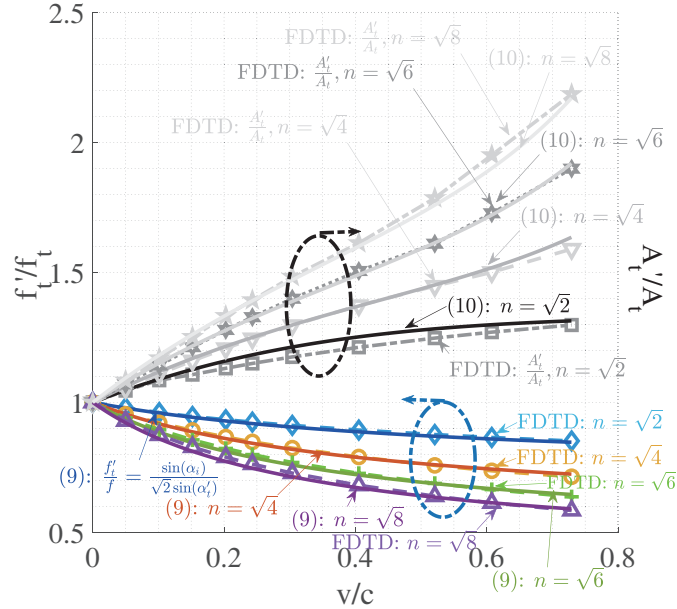


Figure 9. Simulated amplitude in the frequency domain and frequency of transmitted waves, for dielectric interface moving toward the source, with incidence angle $\alpha_i = 45^\circ$, versus $\frac{v}{c}$, for different values of n . Comparison with derived analytical formulas.

wave is given by:

$$\begin{aligned} \frac{A'_t}{A_t} = & \frac{\sin\left(\frac{\alpha'_{r2} + (n-1)\alpha_i}{n} + \alpha'_t + \alpha'_r\right)}{\sin\left(\frac{\alpha'_{r2} + (n-1)\alpha_i}{n} + \alpha'_t + \alpha'_r\right) + n \sin\left(\alpha'_{r2} + \frac{(n+1)\alpha_i - \alpha'_r}{n}\right)} \times \frac{\sin(\alpha_t + 2\alpha_i) + n \sin(2\alpha_i)}{\sin(\alpha_t + 2\alpha_i)} \\ & \times \frac{n \sin(\alpha'_t)}{\sin(\alpha_i)} \end{aligned} \quad (10)$$

For normal incidence, the Doppler effect formula and the amplitude ratio are simplified by the following formula:

$$\frac{f'_t}{f} = \frac{A_t}{A'_t} = \frac{1 + \frac{v}{c}}{1 + n\frac{v}{c}} \quad (11)$$

4. CONCLUSION

This paper has presented an investigation on a moving dielectric half-space illuminated by a plane wave, at oblique incidence. Based on full-wave simulations, which use the Finite Difference Time Domain method, we have derived several analytical formulas for the amplitudes of the transmitted and reflected waves, the Doppler frequency shifts, and the transmission and reflection angles. For straight interface, our results agree with solutions presented in the literature. For inclined interface, we have derived novel and simple formulas for Doppler effect in reflection and transmission, with graphical representations of the formulas. We have also obtained new solutions for amplitudes of reflection and transmission. Furthermore, we have presented an original analysis of the field distribution for this problem.

In existing methods proposed in the literature, problems with moving bodies in electromagnetism are addressed by using change of reference frames and Voigt-Lorentz transformations. The main challenge of such approach is to implement a relative time in a full-wave simulator and to consider complex problems with, for example, multiple bodies moving at different speeds. In this paper, we apply a direct FDTD method and we assess the effectiveness of this technique by analyzing an electromagnetic problem with moving dielectric half-space. In order to implement the proposed approach, the numerical aspects described in Section 2 need to be considered. The proposed approach is simple, and it can be used to consider multiple objects moving at different speeds. It allows to analyze the effects predicted by Maxwell's equations without relativistic effects and to consider accelerating or rotating objects. We suggest the implementation of the proposed technique in commercial FDTD software.

REFERENCES

1. Yee, K., "Numerical solution of initial boundary value problems involving Maxwell's equations in isotropic media," *IEEE Transactions on Antennas and Propagation*, Vol. 14, No. 3, 302–307, 1966.
2. Taflov, A. and M. E. Brodwin, "Numerical solution of steady-state electromagnetic scattering problems using the time-dependent Maxwell's equations," *IEEE Transactions on Microwave Theory and Techniques*, Vol. 23, No. 8, 623–630, 1975.
3. Reineix, A. and B. Jecko, "Analysis of microstrip patch antennas using finite difference time domain method," *IEEE Transactions on Antennas and Propagation*, Vol. 37, No. 11, 1361–1369, 1989.
4. Sheen, D. M., S. M. Ali, M. D. Abouzahra, and J.-A. Kong, "Application of the three-dimensional finite-difference time-domain method to the analysis of planar microstrip circuits," *IEEE Transactions on Microwave Theory and Techniques*, Vol. 38, No. 7, 849–857, 1990.
5. Yee, K. S., D. Ingham, and K. Shlager, "Time-domain extrapolation to the far field based on FDTD calculations," *IEEE Transactions on Antennas and Propagation*, Vol. 39, No. 3, 410–413, 1991.
6. Rabbani, M. S., J. Churm, and A. P. Feresidis, "Fabry-Pérot beam scanning antenna for remote vital sign detection at 60 GHz," *IEEE Transactions on Antennas and Propagation*, Vol. 69, No. 6, 3115–3124, 2021.
7. Chioukh, L., H. Boutayeb, D. Deslandes, and K. Wu, "Noise and sensitivity of harmonic radar architecture for remote sensing and detection of vital signs," *IEEE Transactions on Microwave Theory and Techniques*, Vol. 62, No. 9, 1847–1855, 2014.
8. Taravati, S. and A. A. Kishk, "Space-time modulation: Principles and applications," *IEEE microwave magazine*, Vol. 21, No. 4, 30–56, 2020.
9. Kashaninejad-Rad, A., A. Abdolali, and M. M. Salary, "Interaction of electromagnetic waves with a moving slab: Fundamental dyadic method," *Progress In Electromagnetics Research B*, Vol. 60, 2014.

10. Stolyarov, S., "Reflection and transmission of electromagnetic waves incident on a moving dielectric slab," *Radiophysics and Quantum Electronics*, Vol. 10, No. 2, 151–153, 1967.
11. Yeh, C. and K. Casey, "Reflection and transmission of electromagnetic waves by a moving dielectric slab," *Physical Review*, Vol. 144, No. 2, 665, 1966.
12. Yeh, C., "Propagation along moving dielectric wave guides," *JOSA*, Vol. 58, No. 6, 767–770, 1968.
13. Yeh, C., "Brewster angle for a dielectric medium moving at relativistic speed," *Journal of Applied Physics*, Vol. 38, No. 13, 5194–5200, 1967.
14. Pelosi, G., R. Coccioli, and R. Graglia, "A finite-element analysis of electromagnetic scattering from a moving dielectric cylinder of arbitrary cross section," *Journal of Physics D: Applied Physics*, Vol. 27, No. 10, 2013, 1994.
15. Harfoush, F., A. Tafflove, and G. A. Kriegsmann, "A numerical technique for analyzing electromagnetic wave scattering from moving surfaces in one and two dimensions," *IEEE Trans. on Ant. and Propag.*, Vol. 37, No. 1, 55–63, 1989.
16. Inman, M. J., A. Z. Elsherbeni, and C. Smith, "Finite difference time domain simulation of moving objects," *Proc. of IEEE Radar Conf.*, 2003, 439–445.
17. Zheng, K., X. Liu, Z. Mu, and G. Wei, "Analysis of scattering fields from moving multilayered dielectric slab illuminated by an impulse source," *IEEE Antennas and Wireless Propagation Letters*, Vol. 16, 2130–2133, 2017.
18. Zheng, K.-S., J.-Z. Li, G. Wei, and J.-D. Xu, "Analysis of doppler effect of moving conducting surfaces with lorentz-fdtd method," *Journal of Electromagnetic Waves and Applications*, Vol. 27, No. 2, 149–159, 2013.
19. Liu, Y., K. Zheng, Z. Mu, and X. Liu, "Reflection and transmission coefficients of moving dielectric in half space," *2016 11th International Symposium on Antennas, Propagation and EM Theory (ISAPE), IEEE*, 485–487, 2016.
20. Zheng, K., Z. Mu, H. Luo, and G. Wei, "Electromagnetic properties from moving dielectric in high speed with lorentz-fdtd," *IEEE Antennas and Wireless Propagation Letters*, Vol. 15, 934–937, 2015.
21. Li, Y., K. Zheng, Y. Liu, and L. Xu, "Radiated fields of a high-speed moving dipole at oblique incidence," *2017 International Applied Computational Electromagnetics Society Symposium (ACES), IEEE*, 1–2, 2017.
22. Zheng, K., Y. Li, X. Tu, and G. Wei, "Scattered fields from a three-dimensional complex target moving at high speed," *2018 International Applied Computational Electromagnetics Society Symposium-China (ACES), IEEE*, 1–2, 2018.
23. Zheng, K., Y. Li, L. Xu, J. Li, and G. Wei, "Electromagnetic properties of a complex pyramid-shaped target moving at high speed," *IEEE Transactions on Antennas and Propagation*, Vol. 66, No. 12, 7472–7476, 2018.
24. Zheng, K., Y. Li, S. Qin, K. An, and G. Wei, "Analysis of micromotion characteristics from moving conical-shaped targets using the lorentz-fdtd method," *IEEE Transactions on Antennas and Propagation*, Vol. 67, No. 11, 7174–7179, 2019.
25. Boutayeb, H., "Numerical methods in electromagnetism: Finite difference time domain method, part 1," DOI: <http://dx.doi.org/10.13140/2.1.1247.3604> 10.13140/2.1.1247.3604.